7-11 july 2019

ICSV26

MONTREAL

A COUPLED FINITE ELEMENT/TRANSFER MATRIX METHOD TO SIMULATE THE INSERTION LOSS OF EARPLUGS IN AN ACOUSTIC TEST FIXTURE

Yu Luan

École de technologie supérieure, Montreal, Quebec, Canada
Email: yu.luan.1@ens.etsmtl.ca

Franck Sgard

IRSST, Montreal, Quebec, Canada

Simon Benacchio

École de technologie supérieure, Montreal, Quebec, Canada

Hugues Nélisse

IRSST, Montreal, Quebec, Canada

Olivier Doutres

École de technologie supérieure, Montreal, Quebec, Canada

Acoustic test fixtures (ATFs) can be used to measure the insertion loss (IL) of earplugs. Reliable numerical modeling of the occluded artificial ear canal of the ATF could be helpful for optimizing the earplug performance during the design phase. This requires the simulation of the IEC 60318-4 occluded ear simulator which is usually based on the classical lumped parameter model (LPM) or complete 3D numerical model. Lumped models are generally accepted to have inherent frequency limitations and cannot properly deal with the thermal and viscous phenomena in certain areas of the simulator. 3D numerical models based on the finite element (FE) or boundary element method are capable of accurately describing the simulator behavior taking thermo-viscous effects into consideration but many dimensional details related to the published numerical models of the IEC 60318-4 simulator remain unspecified. This study proposes a transfer matrix (TM) model of the IEC 60318-4 simulator whose geometry is determined using Computed Tomography scan images. The specific acoustic impedance of certain elements in the simulator model is deduced using the low reduced frequency (LRF) model which has been proved satisfactory to account analytically for thermo-viscous energy losses. The TM model is validated using a 3D FE model of the simulator based on the same geometric dimensions. It is then coupled to a 2D axisymmetric FE model of an ATF ear canal occluded or not by a silicone earplug to simulate the earplug IL. The coupled FE/TM method is found to provide satisfactory IL prediction compared to a complete 3D FE model of the corresponding system. The proposed TM model is also shown to better capture the simulator behavior compared to the classical LPM.

Keywords: earplug, insertion loss, IEC 60318-4 ear simulator, finite element, transfer matrix

1. Introduction

Acoustic test fixtures (ATFs) [1] can be used to assess the insertion loss (IL) of earplugs [2]. They are generally composed of a rigid artificial head and a cylindrical ear canal of constant circular cross-section which is always internally covered with a silicone layer to mimic the human skin [2]. The ATF ear canal is coupled to an IEC 60138-4 occluded ear simulator (formerly known as IEC 711 simulator) [3] which is designed to reproduce the average acoustic impedance of the inner part of the human ear from a reference plane (simulator entrance) to the eardrum [3, 4]. It should be noted that the IEC 60138-4 simulator simulates the acoustic effect of both the middle/inner ears and a portion of the ear canal cavity between the reference plane and eardrum. The sound pressure measured by the recording microphone located at the end of the simulator is as close as possible to that measured at the eardrum of an average human ear. The earplug IL corresponds to the difference between the recorded sound pressure levels without and with the earplug.

Earplugs are usually designed empirically or using simplified models, namely lumped parameter models (LPMs). Such models are generally accepted to have inherent frequency limitations and are not sufficient to describe the full vibro-acoustic behavior of earplugs in a wide frequency range. Therefore, reliable numerical modeling of the occluded ATF ear canal could be helpful for optimizing the earplug performance during the design phase. A few studies have tried to predict the IL of earplugs in an ATF ear canal using the finite element (FE) method [5, 6]. However, the simulation of the IEC 60318-4 ear simulator was based on the classical LPM proposed by [7] which considers the simulator as an equivalent electrical circuit. Besides the aforementioned frequency restrictions, the classical LPM cannot properly deal with the thermal and viscous effects in the narrow areas of the simulator. Alternatively, the low reduced frequency (LRF) model has been proved satisfactory by several investigations to account analytically for thermo-viscous phenomena (e.g., [8, 9]) which is however rarely adopted for the modeling of ear simulators. Furthermore, several studies have been published on the use of the FE or boundary element method to model the IEC 60318-4 simulator [7, 10, 11] but the essential geometric dimensions related to these models remain unspecified.

The goals of this paper are to i) model the IEC 60318-4 occluded ear simulator based on the assessed geometric parameters, with the thermo-viscous energy losses involved in the system properly included and ii) simulate numerically the IL of earplugs in an ATF ear canal through the use of this simulator model. More specifically in this work, a transfer matrix (TM) model of a commercial IEC 60318-4 simulator is proposed based on the key dimensions determined from micro-Computed Tomography (micro-CT) scan images. The specific acoustic impedance of certain elements in the simulator model uses the LRF model to take thermo-viscous effects into account. The TM model is validated using a 3D FE model of the scanned simulator and is compared with the classical LPM. It is then coupled to a 2D axisymmetric FE model of an ATF ear canal occluded or not by a silicone earplug to simulate the earplug IL. The IL simulation result using the coupled FE/TM method is shown to agree well with that obtained by a complete 3D FE model of the corresponding system.

2. Geometry of the ear simulator

The ear simulator adopted is the G.R.A.S. RA0045 (G.R.A.S. Sound & Vibration, Denmark) conforming to IEC 60318-4 [3] (see Fig.1). It is composed of a central cylinder (main cavity) which assimilates a portion of the human ear canal (components 1, 3 and 5). The main cavity is connected to two annular lateral cavities through two narrow slits in which thermo-viscous phenomena should not be neglected approximating the energy losses related to the inner part of the human ear from the eardrum to the inner ear. The first narrow slit is rectangular and the second one is made up of three identical annular
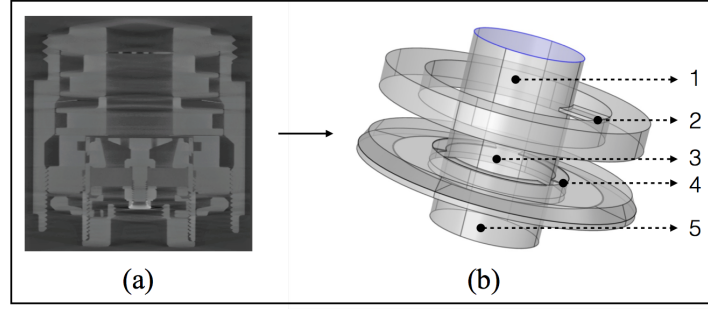
Figure 1: Geometry of the IEC 60318-4 simulator: (a) micro-CT scan image, (b) 3D FE model

components. Moreover, the second lateral volume contains a conical part in which mounted a ring sheet metal. Each lateral cavity and the related slit form a Helmholtz resonator (components 2 and 4). The system is fully fabricated in hard non-porous material and can be considered acoustically rigid. For the sake of simplicity, in this study the recording microphone at the terminal of the simulator is replaced by a rigid boundary since its impedance is sufficiently high compared to the system in front [3]. Key dimensions of the studied IEC 60318-4 simulator are determined using a micro-CT scanner (XT H 225 micro-CT X-Ray Scanner, Nikon Metrology, United States) with a 15.4 μm isotropic resolution and are thereafter used to establish the TM and FE models of the simulator (see Section 3).

3. Modeling strategies of the ear simulator

3.1 Transfer matrix model

The IEC 60318-4 simulator can be modeled analytically through the use of transfer matrices [12], considering only the propagation of plane waves along the axis of revolution in the system given the small sizes of each acoustic element compared to the acoustic wavelength. In this case, the acoustic variables (pressure and particle velocity) at the input and output of each part of the simulator main cavity separated by the narrow slits (see Fig.1(b)) are related by:

$$\boldsymbol{T_{\mathbf{m}}} = \begin{bmatrix} \cos(k_0 L_m) & jZ_0 \sin(k_0 L_m) \\ j\sin(k_0 L_m)/Z_0 & \cos(k_0 L_m) \end{bmatrix} \tag{1}$$

where m=1, 3 and 5 correspond to each part of the main cavity, L_m the length of each part correspondingly, $j = \sqrt{-1}$, k_0 denotes the wavenumber and Z_0 is the characteristic acoustic impedance of air. In the same way, for each Helmholtz resonator (see Fig.1(b)):

$$\boldsymbol{T_{\mathbf{n}}} = \begin{bmatrix} 1 & 0 \\ 0 & S_{slit,n}/S_0 \end{bmatrix} \begin{bmatrix} 1 & 0 \\ 1/Z_{HR,n} & 1 \end{bmatrix} \begin{bmatrix} 1 & 0 \\ 0 & S_0/S_{slit,n} \end{bmatrix} \tag{2}$$

in which n=2 and 4 correspond to the first and second Helmholtz resonators, S_0 and $S_{slit,n}$ are the cross-section areas of the main cavity and narrow slit. $Z_{HR,n}$ denotes the input specific acoustic impedance of the resonator:

$$Z_{HR,n} = Z_{slit,n} + Z_{cav,n} \tag{3}$$

with $Z_{slit,n}$ and $Z_{cav,n}$ the specific impedance values of the slit and the corresponding lateral cavity. It is worth noting that the second lateral cavity is simplified to a pure annular form in the TM model since it

has been proved that only the volume of the cavity affects the simulated impedance of the simulator in the frequency range of interest [100 Hz, 20 kHz]. The specific acoustic impedance of the lateral cavity can be expressed as [8]:

$$Z_{cav,n} = \frac{jZ_0 s_n \left[\dfrac{Y_1(k_0 R_n)}{J_1(k_0 R_n)} J_0(k_0 r_n) - Y_0(k_0 r_n) \right]}{\dfrac{Y_1(k_0 R_n)}{J_1(k_0 R_n)} J_1(k_0 r_n) - Y_1(k_0 r_n)} \tag{4}$$

In the equation above, r_n and R_n denote the inner and outer radii of each cavity, and s_n is the ratio of the slit cross-section area over that of the corresponding lateral cavity. J_0, J_1 and Y_0, Y_1 are Bessel functions of the first and second kind of order 0 and 1. The specific impedance of the slits is deduced from the LRF model which accounts homogeneously for the thermo-viscous effects in the fluid in the form of complex wavenumber and characteristic impedance [8, 9]. For the rectangular slit, one has:

$$Z_{slit,2} = jZ_{l,2} \tan(k_{l,2} a_2) \tag{5}$$

where a_2 is the length of the slit (between the main and lateral cavities), $Z_{l,2}$ and $k_{l,2}$ are the characteristic impedance and wavenumber associated with the LRF model of the rectangular slit [9]. Correspondingly, for the annular slit [8]:

$$Z_{slit,4} = \frac{jZ_{l,4} \left[\dfrac{Y_0(k_{l,4} r_4)}{J_0(k_{l,4} r_4)} J_0(k_{l,4} R_0) - Y_0(k_{l,4} R_0) \right]}{\dfrac{Y_0(k_{l,4} r_4)}{J_0(k_{l,4} r_4)} J_1(k_{l,4} R_0) - Y_1(k_{l,4} R_0)} \tag{6}$$

R_0 and r_4 are the inner and outer radii of the slit, $Z_{l,4}$ and $k_{l,4}$ are the LRF impedance and wavenumber of the annular slit. It is necessary to mention that the end correction of a baffled rectangular piston given in [13] is included in the key dimensions of the narrow slits (a_2, R_0, r_4) to consider the radiation impedance at the related locations. The global TM of the simulator is obtained by combining that corresponding to each component of the system:

$$\boldsymbol{T} = \begin{bmatrix} T_{11} & T_{12} \\ T_{21} & T_{22} \end{bmatrix} = \boldsymbol{T_1} \, \boldsymbol{T_2} \, \boldsymbol{T_3} \, \boldsymbol{T_4} \, \boldsymbol{T_5} \tag{7}$$

The input impedance of the IEC 60318-4 simulator can then be determined from:

$$Z_s = Z_0 \frac{1 + R_s}{1 - R_s} \tag{8}$$

with the simulator reflection coefficient $R_s = (T_{11} - T_{21} Z_0)/(T_{11} + T_{21} Z_0)$.

3.2 Finite element model

In order to validate the TM model, 3D FE modeling of the scanned simulator is performed in COMSOL Multiphysics (v.5.3a COMSOL®, Sweden) similarly as in [11]. The FE model of the IEC 60318-4 simulator is presented in Fig.1(b) with the entrance of the simulator (reference plane) marked in blue. Since the thermo-viscous phenomena in the simulator main cavity and lateral volumes are negligible and those related to the sheet metal in the second lateral cavity have been verified to make no difference on the simulated impedance of the simulator, these domains are governed by Helmholtz equation with no

energy losses. The meshing of these regions is based on quadratic 10-noded tetrahedral elements (at least 6 elements per wavelength). Conversely, thermal and viscous effects are significant in the narrow slits. The sound propagation is then governed by linearized Navier Stokes equations [14]. The mesh density along the horizontal walls of the slits is increased in order to improve the resolution of acoustic boundary layers. The built-in *Acoustics/Thermoviscous Acoustics Multiphysics* coupling condition in COMSOL Multiphysics is used to solve the coupled problem. The system is excited by a displacement of $10^{-5}\ m$ at the reference plane and a rigid terminal boundary condition is adopted. Moreover, the walls of all the simulator components are supposed to be isothermal. The acoustic pressure p and particle velocity $\overrightarrow{v}$ are computed at each node of the reference plane and the input specific impedance of the simulator is obtained by:

$$Z_s = \frac{\int_{S_0} p\,\mathrm{d}S}{\int_{S_0} \overrightarrow{v} \cdot \overrightarrow{n}\,\mathrm{d}S} \tag{9}$$

4. Insertion loss simulation of the earplug

In this section, the TM model of the simulator is coupled to a 2D axisymmetric FE model of an ATF ear canal occluded or not by a silicone earplug to simulate the IL of the earplug. Such ear canal is composed of a rigid cylindrical cavity of circular cross-section terminated by an IEC 60318-4 simulator. Since the objective here is to evaluate the proposed TM model, the earplug lateral walls are supposed to be subjected to a simple "fixed" displacement boundary condition. It should be noted that this boundary condition tends to overestimate the earplug attenuation which can be measured in "real-life" situations or on ATFs because the skin tissues around the ear canal are not accounted for. The coupled FE/TM method is carried out in two steps (see Fig.2). First, the average sound pressure at the reference plane p_1 (in both the open and occluded ear canals) is calculated using the 2D FE model in COMSOL Multiphysics based on the modeling strategy proposed in [5]. The simulator input impedance obtained by the TM model is
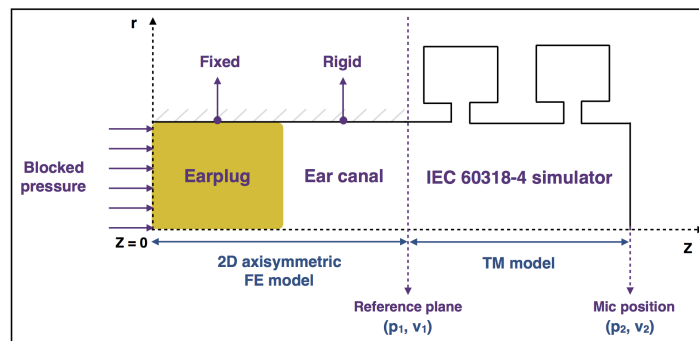

Figure 2: Schematic representation of the coupled FE/TM method

introduced as an impedance boundary condition on the reference plane. A blocked pressure generated by a normal incident plane wave is introduced to the ear canal entrance ($z = 0$). Particularly for the open ear, the radiation impedance of a baffled circular piston is imposed at the same position to account for the interaction with the external sound field [15]. The earplug isotropic elastic material properties used in the model have been determined using a quasi-static mechanical analyzer: Young's modulus ($1.7\ MPa$), Poisson's ratio (0.48), isotropic loss factor (0.18) and density ($1500\ kg \cdot m^{-3}$). In the second step, the corresponding sound pressure at the real microphone position of the simulator (tympanic sound pressure)

p_2 is deduced using the TM model, given that at the reference plane calculated in the previous step. In the case of an infinite terminal impedance of the simulator, this is simply achieved by:

$$p_2 = p_1/T_{11} \tag{10}$$

where T_{11} denotes the first element in the global TM of the simulator (see Eq.7). The IL is defined as the difference between the tympanic sound pressure in the open ear p_2^{op} and that in the ear occluded by the earplug p_2^{oc}:

$$IL = 20\log_{10}(\frac{|p_2^{op}|}{p_{ref}}) - 20\log_{10}(\frac{|p_2^{oc}|}{p_{ref}}) \tag{11}$$

with $p_{ref} = 2 \times 10^{-5} \ Pa$. Furthermore, a complete 3D FE model of the corresponding system is also adopted to simulate directly the average sound pressure at the microphone position p_2 in order to calculate the earplug IL and is compared with the coupled FE/TM method (see Section 5).

5. Results and discussion

Figure 3 displays the simulator input impedance calculated using the TM model (see Eq.8) (solid blue curve) and 3D FE model (see Eq.9) (dashed red curve) in the same frequency range [100 Hz, 20 kHz] as the relevant studies [7, 10, 11]. Particularly in this figure, the impedance determined from the
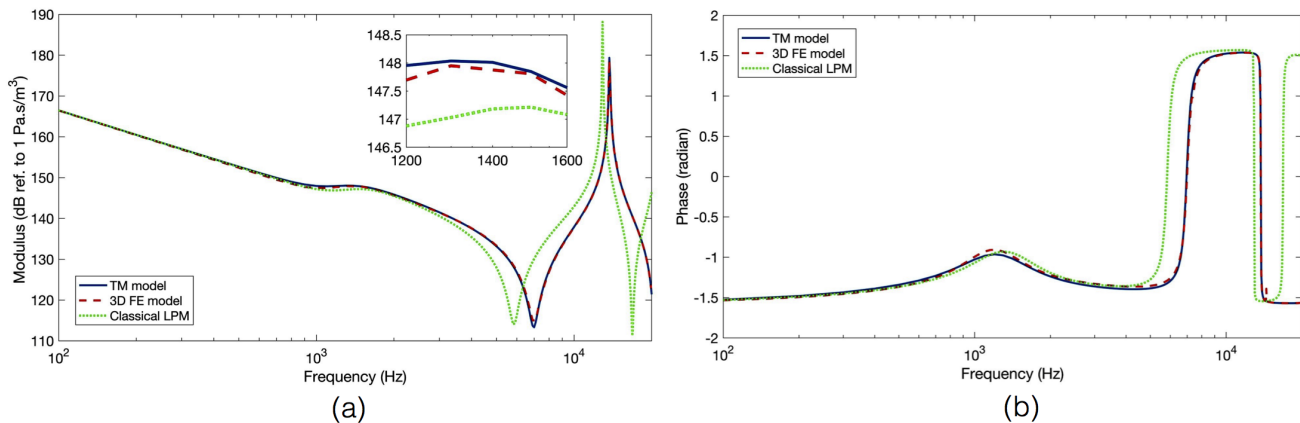

Figure 3: Input impedance of the IEC 60318-4 simulator obtained by different models: (a) modulus, (b) phase

classical LPM of the simulator based on the acquired geometric data (referring to [7] for more details of the method) is also presented for comparison (dashed green line). The result of the TM model is found in perfect accordance with that of the 3D FE model of the simulator in the whole frequency range of interest, which confirms the validity of the former. They both exhibit the first resonance of the simulator main cavity (cylindrical tube of length 13.56 mm) around 13.5 kHz. At frequencies above 3 kHz, the classical LPM proves not to accurately represent the behavior of the IEC 60318-4 simulator compared to the other models due to its inherent frequency limitations. In addition, the mid-frequency behavior of the system is governed by the Helmholtz resonators which have resonant frequencies at respectively 1400 Hz and 3800 Hz. The slight difference between the TM model and classical LPM from 1200 Hz to 1600 Hz (see the "zoomed-in" view of Fig.3(a)) can be explained by the fact that the impedance of the first resonator's neck (rectangular slit) is better captured by the LRF model than the LPM.

Figure 4 illustrates the silicone earplug IL obtained using the coupled FE/TM method (solid blue curve) and 3D FE model of the same configuration as the reference (dashed red curve). Results are displayed in the working frequency range of the IEC 60318-4 simulator [100 Hz, 10 kHz] beyond which it does not necessarily represent the acoustic impedance of the human ear [3]. An excellent correlation is
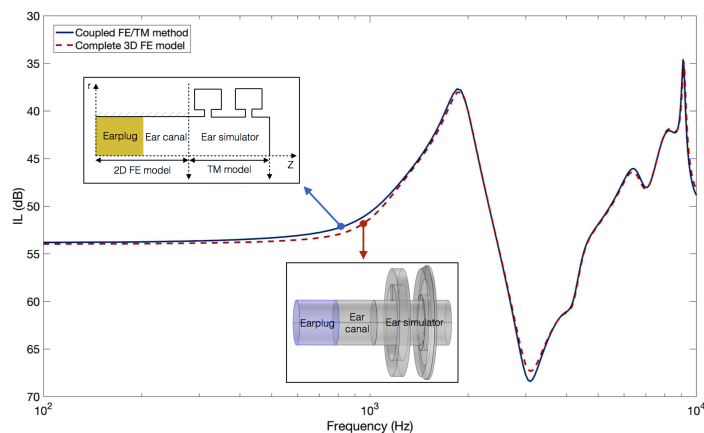

Figure 4: IL of the silicone earplug simulated using different methods

observed between the coupled method and 3D FE model of the system in the frequency range of interest. The peak (minimum attenuation) shown around 1.9 kHz is related to the first mode of the earplug [5, 6]. It corresponds to a longitudinal mode where the outer and inner faces of the earplug vibrate in phase. Other visible peaks in the model correspond to higher vibration modes of the earplug.

6. Conclusion

In this work, a TM model of an IEC 60318-4 occluded ear simulator has been proposed based on a direct determination of the simulator key dimensions from micro-CT scan images. The input impedance of the narrow slits in the simulator was derived through the use of the LRF model to account for thermo-viscous effects. The TM model was validated using a 3D FE model of the scanned simulator in the frequency range [100 Hz, 20 kHz] and was compared with the classical LPM. It was shown to better represent the simulator acoustic impedance at frequencies above 3 kHz compared to the classical LPM. The TM model was then coupled to a 2D axisymmetric FE model of an ATF ear canal occluded or not by a silicone earplug to simulate the earplug IL in the frequency range [100 Hz, 10 kHz]. First, the average sound pressure at the reference plane in both the open and occluded ear canals was calculated using the 2D FE model. In the model, the input impedance of the IEC 60318-4 simulator obtained by the TM model was imposed at the reference plane as an impedance boundary condition. In the second step, the corresponding sound pressure at the microphone position of the simulator was retrieved via the TM model using that acquired in the previous step. The IL simulation result was compared with that obtained by a complete 3D FE model of the corresponding system. The coupled method was found in perfect agreement with the 3D FE model of the system in the frequency range of interest regarding the simulated earplug IL. This demonstrates that the coupled FE/TM method constitutes a reliable alternative for predicting the IL of earplugs in an ATF ear canal up to 10 kHz to the detailed 3D FE modeling of the system. Future work will concentrate on the validation of the IEC 60318-4 simulator impedance model and the earplug IL prediction model using experimental measurements.

REFERENCES

1. ANSI/ASA S3.36-2012. American National Standard Specification for a Manikin for simulated in-situ Airborne Acoustic Measurements. Standard, American National Standards Institute, 2012.

2. ANSI/ASA S12.42-2010. Methods for the measurement of insertion loss of hearing protection devices in continuous or impulsive noise using microphone-in-real-ear or acoustic test fixture procedures. Standard, American National Standards Institute, 2010.

3. IEC 60318-4: 2010. Simulators of human head and ear-Part 4: Occluded-ear simulator for the measurement of earphones coupled to the ear by means of ear inserts. Standard, International Electrotechnical Commission, 2010.

4. ANSI/ASA S3.25-2009. American National Standard for an Occluded Ear Simulator. Standard, American National Standards Institute, 2009.

5. G. Viallet, F. Sgard, F. Laville, and J. Boutin. Axisymmetric versus three-dimensional finite element models for predicting the attenuation of earplugs in rigid walled ear canals. *The Journal of the Acoustical Society of America*, 134(6):4470–4480, 2013.

6. G. Viallet, F. Sgard, F. Laville, and J. Boutin. A finite element model to predict the sound attenuation of earplugs in an acoustical test fixture. *The Journal of the Acoustical Society of America*, 136(3):1269–1280, 2014.

7. L. Nielsen, A. Schuhmacher, B. Liu, and S. Jonsson. Simulation of the IEC 60711 occluded ear simulator. In *Audio Engineering Society Convention 116*. Audio Engineering Society, 2004.

8. D. Rodrigues, C. Guianvarcâh, J.-N. Durocher, M. Bruneau, and A.-M. Bruneau. A method to measure and interpret input impedance of small acoustic components. *Journal of Sound and Vibration*, 315(4-5):890–910, 2008.

9. W. R. Kampinga. *Viscothermal acoustics using finite elements-Analysis tools for engineers*. PhD thesis, 2010.

10. M. Sasajima, T. Yamaguchi, M. Watanabe, and Y. Koike. FEM Analysis of Occluded Ear Simulator with Narrow Slit Pathway. *International Journal of Mechanical, Aerospace, Industrial, Mechatronic and Manufacturing Engineering*, 9(9):1430–1433, 2015.

11. COMSOL Multiphysics 5.3a. Generic 711 Coupler - An Occluded Ear Canal Simulator. `https://www.comsol.com/model/generic-711-coupler-8212-an-occluded-ear-canal-simulator-12227`, 2017.

12. J. F. Allard and N. Atalla. *Propagation of sound in porous media: modelling sound absorbing materials 2e*. John Wiley & Sons, 2009. pp. 243–280.

13. M. L. Munjal, M. Vorländer, P. Költzsch, M. Ochmann, A. Cummings, W. Maysenhölder, and W. Arnold. *Formulas of acoustics*. Springer Science & Business Media, 2008. p. 319.

14. D. T. Blackstock. *Fundamentals of physical acoustics*. John Wiley & Sons, 2000. pp. 298–327.

15. J. Schroeter and C. Poesselt. The use of acoustical test fixtures for the measurement of hearing protector attenuation. Part II: Modeling the external ear, simulating bone conduction, and comparing test fixture and real-ear data. *The Journal of the Acoustical Society of America*, 80(2):505–527, 1986.